Journal of Controlled Release 331 (2021) 376–389

Contents lists available at ScienceDirect

Journal of Controlled Release

journal homepage: www.elsevier.com/locate/jconrel

Oxygen-release microspheres capable of releasing oxygen in response to environmental oxygen level to improve stem cell survival and tissue regeneration in ischemic hindlimbs

Ya Guan [a,b,1], Ning Gao [a,b,1], Hong Niu [a,b], Yu Dang [a,b], Jianjun Guan [a,b,*]

[a] Department of Mechanical Engineering and Materials Science, Washington University in St. Louis, St. Louis, MO 63130, USA
[b] Department of Materials Science and Engineering, The Ohio State University, Columbus, OH 43210, USA

ARTICLE INFO

Keywords:
Critical limb ischemia
Stem cell therapy
Oxygenation
Angiogenesis
Skeletal muscle regeneration

ABSTRACT

Stem cell transplantation has been extensively explored to promote ischemic limb vascularization and skeletal muscle regeneration. Yet the therapeutic efficacy is low due to limited cell survival under low oxygen environment of the ischemic limbs. Therefore, continuously oxygenating the transplanted cells has potential to increase their survival. During tissue regeneration, the number of blood vessels are gradually increased, leading to the elevation of tissue oxygen content. Accordingly, less exogenous oxygen is needed for the transplanted cells. Excessive oxygen may induce reactive oxygen species (ROS) formation, causing cell apoptosis. Thus, it is attractive to develop oxygen-release biomaterials that are responsive to the environmental oxygen level. Herein, we developed oxygen-release microspheres whose oxygen release was controlled by oxygen-responsive shell. The shell hydrophilicity and degradation rate decreased as the environmental oxygen level increased, leading to slower oxygen release. The microspheres were capable of directly releasing molecular oxygen, which are safer than those oxygen-release biomaterials that release hydrogen peroxide and rely on its decomposition to form oxygen. The released oxygen significantly enhanced mesenchymal stem cell (MSC) survival without inducing ROS production under hypoxic condition. Co-delivery of MSCs and microspheres to the mouse ischemic limbs ameliorated MSC survival, proliferation and paracrine effects under ischemic conditions. It also significantly accelerated angiogenesis, blood flow restoration, and skeletal muscle regeneration without provoking tissue inflammation. The above results demonstrate that the developed microspheres have potential to augment cell survival in ischemic tissues, and promote ischemic tissue regeneration in a safer and more efficient manner.

1. Introduction

Peripheral artery disease (PAD), which affects more than 200 million people worldwide, is a progressive atherosclerotic disorder induced mainly by the lipid deposition in the vascular bed as a result of hardening and narrowing of arteries [1]. Approximately 10% of the PAD patients develop critical limb ischemia (CLI), with 30% of them gain limited outcomes from conservative therapies and have no choice but leg amputation [2]. CLI is characterized by low blood perfusion, severe tissue ischemia and degenerated skeletal muscle, which lead to non-healing wounds, ulcers and necrosis in the terminal stage [3,4]. Thus, quick restoration of blood perfusion to rescue existing tissue and acceleration of muscle repair represent the major goals for CLI treatment.

Conventional treatments for CLI include arterial bypass and endovascular therapy. However, these therapeutic approaches are rather invasive, and are not suitable for CLI patients with severe comorbidity or sepsis [5,6]. There has been extensive interest in alternative approaches to address current limitations, such as proangiogenic growth factor therapy [7], gene therapy [8], and stem cell therapy [9]. Compared to growth factor and gene therapies, stem cell therapy has advantages. The delivered stem cells may secrete a wide range of growth factors that are necessary for the blood vessel formation and/or myogenesis [10,11]. The stem cells may also have the capacity of differentiating into

* Corresponding author at: Department of Mechanical Engineering and Materials Science, Washington University in St. Louis, 303F Jubel Hall (Office), 340 Whitaker Hall (Lab), Campus Box 1185, One Brookings Drive, St. Louis, MO 63130, United States of America.
E-mail address: jguan22@wustl.edu (J. Guan).
[1] These authors contributed equally to this work.

https://doi.org/10.1016/j.jconrel.2021.01.034
Received 13 August 2020; Received in revised form 20 January 2021; Accepted 21 January 2021
Available online 27 January 2021

endothelial cells for vascularization [10,12,13]. Therefore, stem cell therapy possesses greater potentials than the other approaches in promoting ischemic tissue regeneration [6].

Various stem cell types including adipose-derived stem cells [14,15], mesenchymal stem cells (MSCs) [16–18], iPSC-derived mesenchymal stem cells [19], ESC-derived stem cells [20,21] have been tested for ischemic limb regeneration. Among them, MSCs are considered as potent biofactories, which improve the angiogenesis and myogenesis by secreting various types of angiogenic and myogenic factors [22]. These include vascular endothelial growth factor (VEGF), platelet-derived growth factor (PDGF), basic fibroblast growth factor (bFGF), hepatocyte growth factor (HGF), and insulin-like growth factor-1 (IGF-1). These growth factors are also of particular interest in the growth factor therapy [23]. Another key advantage of MSCs is that they perform immunoregulatory function via producing soluble factors that regulate immune response, such as PEG2 and IL-6 [24]. In addition, MSCs promote angiogenesis by acting as pericytes [25–27], and/or providing an appropriate microenvironment for cell types like endothelial cells to form blood vessels [28].

Although MSCs exhibit promising potentials in accelerating angiogenesis and myogenesis, clinical trials only showed low efficiency in the improvement of blood perfusion and muscle repair [29]. One of the key causes is the poor cell survival and engraftment under low oxygen condition of the ischemic limbs [30,31]. Accordingly, we hypothesized that co-delivery of oxygen-release biomaterials and MSCs may increase cell survival and engraftment by continuously oxygenating the delivered cells. The released oxygen may also support host cells to survive and proliferate. The enhanced cell survival would promote ischemic tissue vascularization and myogenesis.

To improve cell survival under ischemia by continuous supply of oxygen, various oxygen-release systems have been developed. They were based on H_2O_2 [32,33], CaO_2 [34] and fluorinated molecules [35,36]. Current oxygen release systems typically release oxygen for less than two weeks [32–36], thus are unable to support long-term cell survival in ischemic limbs [37,38], since the establishment of angiogenesis needs more than 3 weeks [39,40]. To address this limitation, we have recently developed novel oxygen-release microspheres (ORM) based on polyvinylpyrrolidone (PVP)/H_2O_2 complex, poly(lactide-*co*-glycolide) (PLGA) and catalase [41–43]. We have shown that the high-molecular-weight PVP/H_2O_2 can gradually release from the PLGA shell and convert to molecular oxygen by catalase. The duration of the oxygen release can reach up to 4 weeks, which has been proved to augment cardiac cell survival when transplanted into the ischemic hearts [41]. While these findings are promising, the current oxygen release systems cannot release oxygen in response to tissue oxygen level [41–43]. During tissue regeneration, the number of blood vessels are gradually increased, leading to the elevation of tissue oxygen content. Accordingly, less exogenous oxygen is needed for the transplanted cells. Excessive oxygen may induce reactive oxygen species (ROS) formation, causing cell apoptosis [44–47]. Thus, it is attractive to develop oxygen-release systems that are responsive to the environmental oxygen level.

In this work, we developed new microspheres capable of releasing oxygen depending on the environmental oxygen level, i.e., releasing faster at a lower environmental oxygen level, while releasing slower at a higher environmental oxygen level. The microspheres had an oxygen-responsive shell that contained 2-nitroimidazole whose hydrophilicity increases when the environmental oxygen level decreases [48,49]. This enabled the shell to have higher hydrophilicity and degradation rate, leading to faster oxygen release. The shell was also conjugated with catalase on the surface, allowing the microspheres to directly release molecular oxygen. These microspheres are safer than those existing oxygen-release biomaterials that release hydrogen peroxide and rely on its decomposition to form oxygen [32,33]. Hydrogen peroxide may damage the cells when it is not timely decomposed [50]. We investigated the oxygen release kinetics at different environmental oxygen content, and the efficacy of the released oxygen in enhancing MSC survival under hypoxia in vitro. We further transplanted the oxygen-release microspheres and MSCs into ischemic limbs and evaluated the survival and proliferation of MSCs, tissue angiogenesis, skeletal muscle regeneration, and tissue inflammatory response.

2. Materials and methods

2.1. Materials

All chemicals were purchased from Sigma-Aldrich unless otherwise stated. N-isopropylacrylamide (NIPAAm, TCI) was recrystallized in hexane for 3 times before use. 2-Hydroxyl methacrylate (HEMA, Alfa Aesar) was passed through inhibitor removers. Hydrogen peroxide (30 wt% in water), PVP (40 kDa, Fisher Scientific), bovine liver catalase (2000–5000 units/mg), tris(4,7-diphenyl-1,10-phenanthroline) ruthenium (II) dichloride ($Ru(Ph_2phen_3)Cl_2$, GFS chemicals) were used as received.

2.2. Synthesis of 2-(2-nitroimidazolyl) ethanamine (NIEM)

NIEM was synthesized in order to conjugate it to the microspheres so as to impart the microsphere shell with oxygen sensitivity (Fig. 2A). Briefly, 2-bromoethylamine hydrobromide (1.0 equiv), di-tert-butyl dicarbonate (Boc_2O, 1.1 equiv) and 4-dimethylaminopyridine (DMAP, 0.2 equiv) were dissolved in dichloromethane (DCM) at 0 °C. Triethylamine (TEA, 1.1 equiv) was added dropwise to the solution. After overnight stirring at room temperature, the mixture was rinsed subsequently with saturated NH_4Cl, $NaHCO_3$ and NaCl. The organic layer was dried over anhydrous Na_2SO_4 and evaporated to obtain tert-butyl (2-bromoethyl) carbonate. Then, tert-butyl (2-bromoethyl) carbonate (1.1 equiv) and 2-nitroimidazole (1.0 equiv) were dissolved in dimethylformamide in the presence of K_2CO_3 (1.5 equiv) and NaI (0.2 equiv). The reaction was conducted at 80 °C for 4 h followed by overnight stirring at room temperature. The product was dissolved in ethyl acetate, rinsed sequentially with saturated $NaHCO_3$ and NaCl, dried over anhydrous Na_2SO_4, and filtered. The filtrate was concentrated and purified by flash chromatography using ethyl acetate/hexane (1/1). Finally, the product was dissolved in DCM/trifluoroacetic acid, and stirred overnight at room temperature to deprotect the amine group and obtain NIEM. The chemical structure of NIEM was confirmed by ^1H NMR ($(CD_3)_2SO$): δ 7.64 (d, 1H), 7.23 (d, 1H), 4.62–4.65 (t, 2H), 3.32–3.35 (t, 2H)).

2.3. Synthesis of microsphere shell

The microsphere shell was based on NIPAAm, HEMA, acrylate-oligolactide (AOLA) and N-acryloxysuccinimide (NAS). AOLA and NAS were synthesized as previously reported [41,42,51]. The polymer poly (NIPAAm-*co*-HEMA-co-AOLA-co-NAS) (abbreviated as PNHAN) was synthesized by free radical polymerization using benzoyl peroxide as an initiator (Fig. 2B) [41,51–53]. The feed ratio of NIPAAm/HEMA/AOLA/NAS was 50/5/25/20. The reaction was performed at 70 °C for 20 h under the protection of nitrogen. The polymer was precipitated in hexane, and purified three times by dissolving in tetrahydrofuran and precipitating in ethyl ether. The hydrogel poly(NIPAAm-*co*-HEMA-co-AOLA) (abbreviated as PNHA) was synthesized using the same polymerization method with a feed ratio of NIPAAm/HEMA/AOLA = 86/10/4. This hydrogel was used to deliver microspheres and MSCs into ischemic limbs.

2.4. Conjugation of NIEM with PNHAN

NIEM was conjugated to the polymer by reacting with the succinimide group in NAS component (Fig. 2B). Briefly, PNHAN, NIEM, and TEA were dissolved in dimethylformamide and mixed together. The reaction was conducted at 60 °C overnight. After the solvent was

evaporated, the product was purified 3 times by dissolving in tetrahydrofuran and precipitating in ethyl ether. PNHAN with different NIEM contents were obtained by changing the ratio of PNHAN and NIEM. The NIEM conjugated polymer was abbreviated as PNHAN/NIx where x represents the ratio of 2-nitroimidazolyl (NI) group.

2.5. Characterization of the hypoxia-sensitive polymer

Chemical structures of the polymer before and after NIEM conjugation were confirmed by ^{1}H NMR. Polymer composition was calculated from the spectra. Water content and degradation of PNHAN with different NIEM contents were conducted in Dulbecco's phosphate-buffered saline (DPBS, Thermo Fisher) under normoxia (21% O_2) and hypoxia (1% O_2), respectively. Briefly, the polymer was dissolved in DCM, and added into a 1.5 mL centrifuge tube. After solvent evaporation, 200 μL of DPBS was added. DPBS was supplemented with 1% penicillin/streptomycin (Thermo Fisher) to prevent the growth of bacteria. After 12 h of incubation at 37 °C, the hydrated weight of polymer film was measured (w_1). The polymer film was then lyophilized and the dry weight was measured (w_2). The water content was calculated as $(w_1-w_2)/w_2 \times 100\%$.

For degradation study, the polymer films were incubated in DPBS under normoxia (21% O_2) and hypoxia (1% O_2) for 8 weeks, respectively. At each time point, the samples ($n = 4$ for each group) were taken out, washed with DI water, and lyophilized. The sample weight was then measured. The percentage of weight remaining was calculated as weight at each time point normalized to the weight before degradation.

2.6. Fabrication and characterization of oxygen-release microspheres

The oxygen-release microspheres were fabricated by coaxial electrospraying. NIEM conjugated PNHAN, and PVP/H_2O_2 were used as shell and core, respectively. Blends of PNHAN and PNHAN/NI18 with molar ratio of 0, 3/7 and 9/1 were dissolved in DCM at a concentration of 5 wt%. The NI content in the polymer shell was 0, 5% and 16%, respectively. PVP was dissolved in 30% H_2O_2. The molar ratio of H_2O_2 and repeating unit vinylpyrrolidone (VP) was controlled at 4.5/1. The flow rates of the PVP/H_2O_2 complex and PNHAN solution were 0.2 and 1 mL/h, respectively. The coaxial device was charged at a voltage of +15 kV. The microspheres were collected on a rotating mandrel covered with aluminum foil charged at −10 kV. Following fabrication, the microspheres were lyophilized and stored at −20 °C before use. To visualize the core-shell structure of the microspheres, rhodamine B and fluorescein isothiocyanate (FITC) were added to the PNHAN solution and PVP/H_2O_2 solution, respectively. The fluorescent images were taken right after microsphere fabrication using a confocal microscope (Olympus FV1200) to avoid the diffusion of fluorescent dyes. To characterize morphology and size of the microspheres, scanning electron microscopy (SEM) was used.

The microspheres were further conjugated with catalase so that the released PVP/H_2O_2 can be timely converted into oxygen at the microsphere surface. In brief, 50 mg of oxygen-release microspheres were mixed with 6 mL catalase solution (5 mg/mL in DI water), and stirred for 4 h at 4 °C. The mixture was then centrifuged. The microspheres were washed 3 times with DI water to remove un-conjugated catalase. To confirm the conjugation, catalase was pre-labeled with FITC, and fluorescent images were taken using a confocal microscope (Olympus FV1200). The microspheres without catalase conjugation were used as control. The catalase conjugation efficiency was determined by measuring the fluorescent intensity of the microspheres and converting the fluorescent intensity into catalase concentration using a calibration curve.

2.7. Characterization of oxygen release kinetics under different environmental oxygen level

The oxygen release kinetics was tested under 1% or 5% oxygen condition for 28 days. PDMS membrane encapsulated with an oxygen-sensitive luminophore $Ru(Ph_2phen_3)Cl_2$ and an oxygen-insensitive dye rhodamine B was placed in a 96-well plate [54]. Rhodamine B was used as a reference. 200 μL of DPBS was then added into each well. The plate was placed under 1% or 5% oxygen condition for 24 h followed by adding 50 mg of dry microspheres into each well under corresponding oxygen condition ($n = 8$ for each group). At each time point, the fluorescence intensity was measured for $Ru(Ph_2phen_3)Cl_2$ ($\lambda_{excitation} = 470$ nm, $\lambda_{emission} = 610$ nm) and rhodamine B ($\lambda_{excitation} = 543$ nm, $\lambda_{emission} = 576$ nm) using a fluorescent plate reader (Molecular Devices). The oxygen level measured by $Ru(Ph_2phen_3)Cl_2$ represented the oxygen content in PDMS membrane in real-time. A calibration curve was used to convert the fluorescence intensity to oxygen level (**Appendix. 1**). The residual H_2O_2 concentration in the release medium was determined by Pierce peroxide assay (Thermo Fisher).

To evaluate bioactivity of the conjugated catalase, oxygen release from the microspheres with catalase conjugation, and from the microspheres incubated in the release medium containing the same amount of free catalase (260 $\mu g_{catalase}/mg_{microsphere}$) was measured, respectively.

2.8. MSC survival, ROS content, and cellular oxygen level measurement

Rat mesenchymal stem cells (Cell Applications) were cultured in minimum essential medium alpha (αMEM, Thermo Fisher) supplemented with 10% fetal bovine serum (FBS, Corning) and 1% penicillin/streptomycin. To investigate the effect of oxygen release on MSC survival under hypoxia, 50 mg/mL of microspheres and 2 million/mL MSCs were encapsulated in 4 wt% PNHA hydrogel at 4 °C. The mixture was placed in a 37 °C incubator for gelation. Then, the supernatant was replaced by serum-free αMEM medium pre-incubated in 1% O_2 condition. The constructs were cultured in a 1% O_2 incubator. At each time point, the constructs ($n = 4$ for each group) were digested by papain solution at 60 °C. The double stranded DNA (dsDNA) content was measured using a PicoGreen dsDNA assay kit (Thermo Fisher). To visualize the live cells, MSCs were pre-labeled with a live cell tracker, CM-Dil (Thermo Fisher). To determine cell ROS expression, MSCs were pre-stained with CM-H_2DCFDA (Thermo Fisher). Fluorescent images were taken using a confocal microscope.

Electron paramagnetic resonance (EPR) was used to determine intracellular oxygen content. Briefly, MSCs were incubated with lithium phthalocyanine (LiPc) nanoparticles (10 mg/mL in αMEM) for 1 h to allow cellular uptake. The cells were then washed with DPBS for 3 times to remove the free LiPc nanoparticles from cell surface. After trypsinization, the cells (2 million/mL) and microspheres (50 mg/mL) were encapsulated in the PNHA gel (4 wt%). The constructs were loaded into EPR tubes ($n = 3$ for each group). The tubes were placed in a hypoxic incubator (1% O_2, 37 °C) for 48 h. The EPR tests were performed on an X-band EPR instrument (Bruker), with 0.1 mW for microwave power, 1.0 dB for attenuation, 9.8 GHz for frequency, and 1.5 for modulation amplitude [52]. The intracellular oxygen content was determined based on the linewidth of samples, and calibration curve of linewidth vs. oxygen content.

2.9. Implantation of oxygen-release microspheres and MSCs into mouse ischemic limbs

All animal care and experiment procedures were conducted in accordance with the National Institutes of Health guidelines. The animal protocol was approved by the Institutional Animal Care and Use Committee of The Ohio State University. Wild type C57BL/6 mice (Charles River Laboratories) at the age of 8–10 weeks were used. Ischemic surgery was performed on one hindlimb, and the contralateral hindlimb

was used as control. To induce ischemia, unilateral femoral artery and vein were ligated and cut (Fig. 1). Thirty minutes later, 4 wt% PNHA solution (Gel group), or PNHA solution with 2 million cells/mL CMDil-labeled MSCs (Gel/MSC group), or PNHA solution with 2 million cells/mL CMDil-labeled MSCs and 50 mg/mL oxygen-release microspheres (Gel/MSC/ORM group) was injected to the gracilis muscle. Four injections were made for each ischemic hindlimb (50 μL/injection). Six mice were used for each group. At days 1, 7, 14, 21 and 28, the blood perfusion of the normal and surgery hindlimbs was measured using a laser Doppler perfusion imager (Perimed). The blood flow recovery percentage was calculated by normalizing the blood perfusion intensity in the ischemic hindlimb to the normal hindlimb in the same animal [55].

2.10. Histology and immunohistochemical staining

Four weeks after surgery, the mice were euthanized. The hindlimbs with and without surgery were collected. The tissues were fixed with 4% paraformaldehyde for 48 h, embedded in paraffin, and sectioned into 5-μm slices. The CM-Dil + MSCs were imaged using a confocal microscope. Cell density was then quantified from the images. For histological assessment of skeletal muscle, hematoxylin and eosin (H&E) staining was performed. Muscle fiber diameter, and density of central nucleus in muscle fibers were quantified based on the H&E images. For immunohistochemical analysis, the tissue sections were first stained with anti-alpha smooth muscle actin-alpha (α-SMA, Abcam), isolectin (Thermo Fisher), anti-Ki67 (Thermo Fisher), anti-myosin heavy chain (MHC, R&D) and anti-F4/80 (Santa Cruz Biotechnology), respectively. The tissue sections were then incubated with corresponding Dylight488-anti mouse and 647-anti rabbit secondary antibodies. Cell nuclei were stained with Hoechst 33342 or DRAQ5. Immunofluorescence images were taken with a confocal microscope (Zeiss LSM700). Proliferating MSCs were identified as those CMDil+ and Ki67+ cells. Blood vessels were isolectin+ lumens. Mature blood vessels were lumens positive to both isolectin and α-SMA.

2.11. Gene expression of angiogenic and prosurvival growth factors in ischemic limbs

To determine angiogenic and prosurvival growth factor expression in the ischemic limbs with or without implantation of MSCs and oxygen-release microspheres, the expression of bFGF, PDGF-BB and HGF at mRNA level was characterized using real time RT-PCR. RNA was isolated from the ischemic limbs using TRIzol. cDNA was synthesized at 1 μg/reaction using a high capacity cDNA reverse transcription kit (Invitrogen). The primer sequences are listed in **Appendix. 2**. Real-time RT-PCR was conducted using SYBR Green master mix (Invitrogen) on Applied Biosystems™ QuantStudio™ 5 Real-Time PCR System (384-well). The fold of change was calculated using a standard ΔΔCt method ($n \geq 6$ for each group).

2.12. Statistical analysis

All results were presented as mean ± standard deviation. Comparisons among groups were performed using one-way ANOVA with post hoc Tukey test. Statistical significance was set as $p < 0.05$.

3. Results and discussion

3.1. Synthesis and characterization of oxygen-sensitive polymers

The oxygen-sensitive polymers were synthesized by conjugating PNHAM with NIEM. The PNHAM was made by free radical polymerization of NIPAAm, HEMA, AOLA and NAS (Fig. 2B). The molar ratio of the four components was calculated as NIPAAm/HEMA/AOLA/NAS = 52.5/4.4/22.3/20.8 (Fig. 2C), which was consistent with the feed ratio. PNHAN was conjugated with NIEM via the succinimide-amine reaction (Fig. 2B). The conjugation was confirmed by ^{1}H NMR spectrum where the characteristic peak of NAS at 2.8 ppm became unpronounced after conjugation (Fig. 2C). Polymers with 9% and 18% of NI group were synthesized (abbreviated as PNHAN/NI9 and PNHAN/NI18, respectively).

To investigate whether these polymers were responsive to the environmental oxygen level, water content of PNHAN/NI9 and PNHAN/NI18 at both normoxia (21% O_2) and hypoxia (1% O_2) conditions were measured (Fig. 3A). The results demonstrate that PNHAN/NI9 and PNHAN/NI18 exhibited a significantly higher water content under hypoxia than normoxia ($p < 0.01$). This is largely due to the oxygen-dependent reductive reaction which converts the hydrophobic nitro group to the hydrophilic amine group under hypoxia [48,49]. With the increase of NI content from 9% to 18%, the water content of the polymers in hypoxia appeared to have increased, although statistical significance was not reached. The reductive reaction requires a reductant (i.e. an electron donor). In this experiment, glucose, a reducing sugar, in DPBS served as reductant. In the studies with cells, many reductase enzymes produced by cells can act as electron donors, such as xanthine

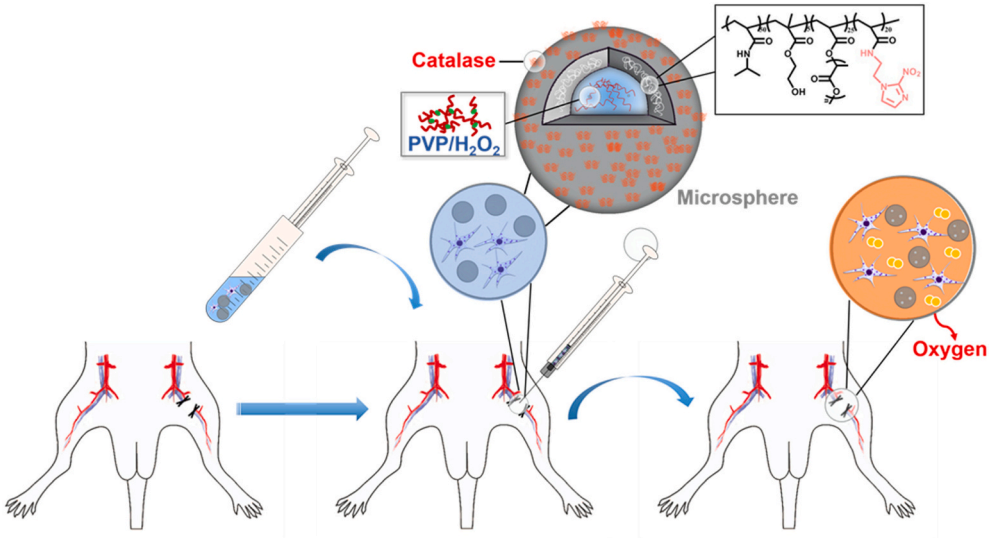

Fig. 1. Scheme of the design of hypoxia-sensitive oxygen-release microspheres and the animal model of critical limb ischemia (CLI).

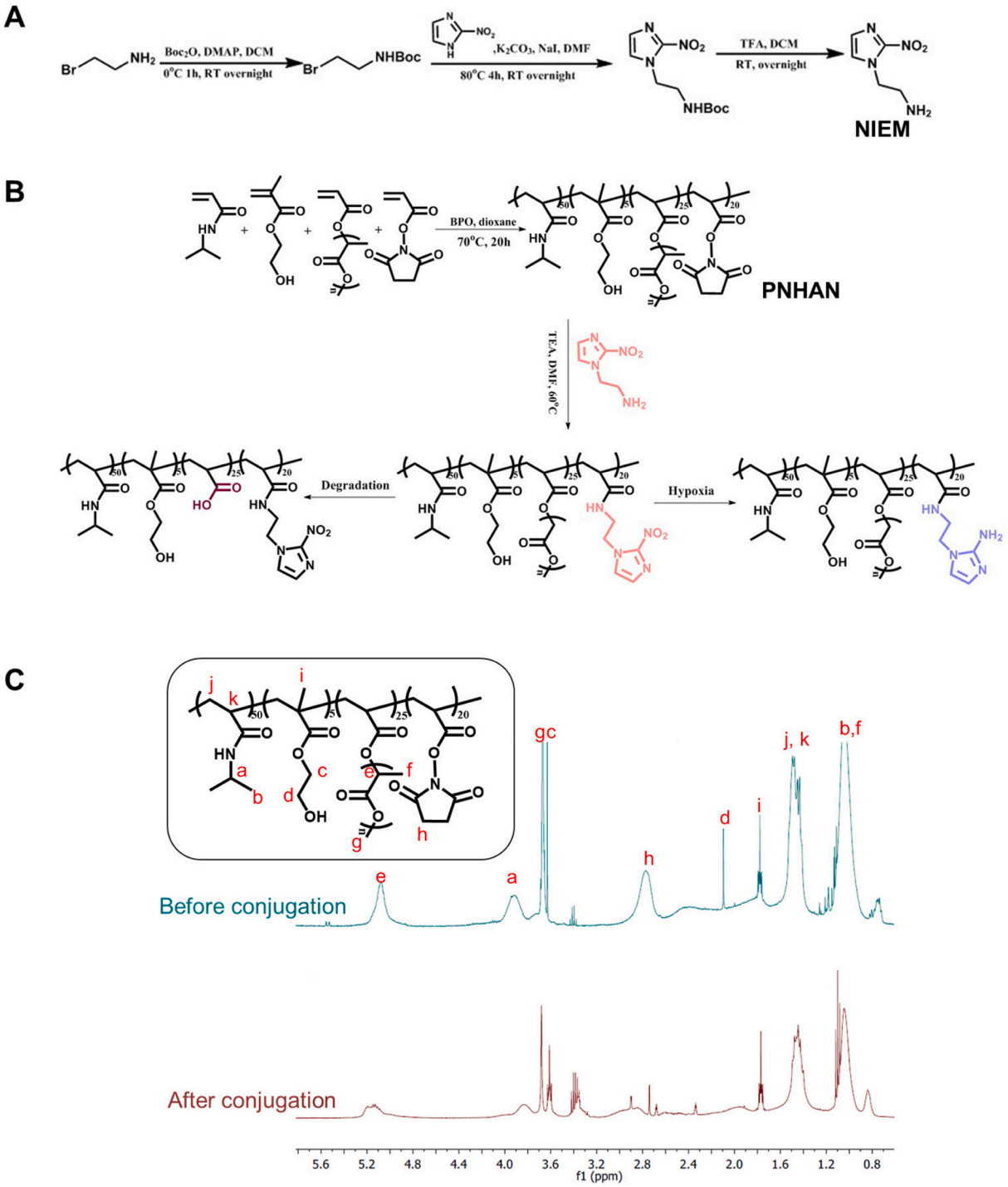

Fig. 2. Synthesis of a hypoxia-sensitive and degradable polymer. (A) Synthesis route of 2-(2-nitroimidazolyl) ethanamine (NIEM); (B) Synthesis of poly(NIPAAm-*co*-HEMA-co-AOLA-co-NAS) (PNHAN), conjugation with NIEM and its degradation mechanism; (C) ^{1}H NMR spectrum of PNHAN and PNHAN/NI18.

oxidase and aldehyde dehydrogenase [48].

We further studied the degradation of oxygen-sensitive polymer (PNHAN/NI9) under normoxia and hypoxia conditions (Fig. 3B). Under aqueous condition, the ester groups in oligolactide can hydrolyze (Fig. 2B). The polymer had 30.7% weight loss after 8 weeks in normoxic environment. The weight loss was significantly increased to 39.2% in hypoxic condition ($p < 0.001$). The higher degradation rate under hypoxia can be attributed to faster hydrolysis caused by enhanced hydrophilicity of the polymer in response to the low oxygen environment. After complete degradation, the resulting polymer was soluble in DPBS at 37 °C, as its gelation temperature was increased to 63 °C, greater than 37 °C. The degraded polymer can thus be eliminated from the body by urinary system in vivo.

3.2. Fabrication and characterizations of oxygen-release microspheres

The oxygen-release microspheres were fabricated by co-axial electrospraying. The microspheres assumed core-shell structure as confirmed by confocal images of the shell and core (Fig. 4A). The diameter was ~5 μm (Fig. 4B). The shell was a blend of PNHAN and PNHAN/NI18. The NHS group in the PNHAN was used to conjugate catalase on the microspheres. The PNHAN/NI18 imparted the

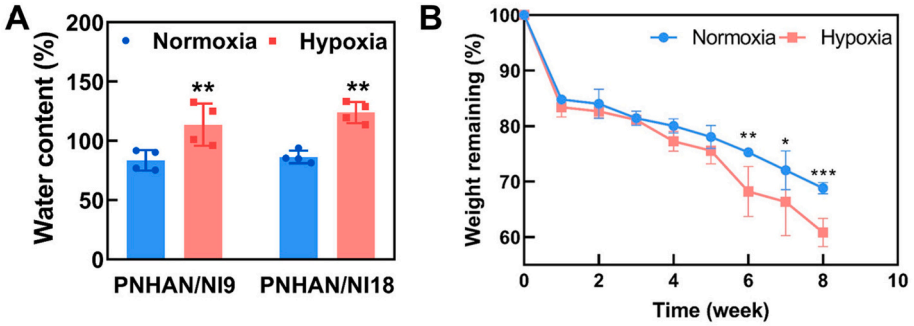

Fig. 3. Characterizations of the polymer under different oxygen content. (A) Water content of the polymer with different NI conjugation ratios under normoxia and hypoxia. The samples were incubated in 37 °C DPBS for 12 h; (B) Degradation of the PNHAN/NI9 polymer under normoxia and hypoxia for 8 weeks. $^{*}p < 0.05$, $^{**}p < 0.01$, $^{***}p < 0.001$.

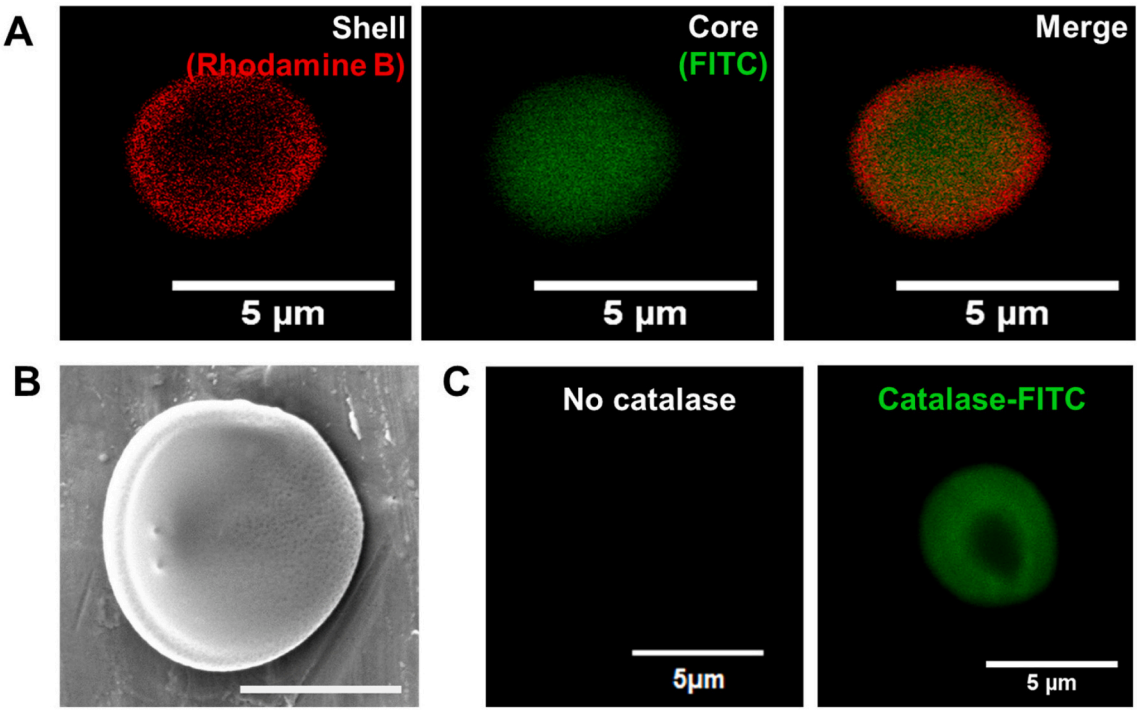

Fig. 4. Characterizations of the oxygen-release microspheres. (A) Fluorescent images of the oxygen-release microspheres. The green fluorescence is FITC added to the core and the red fluorescence is the rhodamine added to the shell; (B) SEM images of the oxygen-release microsphere. Scale bar = 5 μm; (C) Fluorescent image of the oxygen-release microsphere before and after conjugation with FITC-labeled catalase. (For interpretation of the references to colour in this figure legend, the reader is referred to the web version of this article.)

microspheres with oxygen sensitivity. The ratio of PNHAN and PNHAN/NI18 were modulated to allow the shell to have NI content of 5% and 16%, respectively. The core of the microspheres was PVP/H_2O_2 complex. The rationale of using PVP/H_2O_2 complex instead of pure H_2O_2 is that the small molecule H_2O_2 diffuses too fast to achieve long-term oxygen release. Binding H_2O_2 with a high molecular weight PVP can decrease the diffusion rate [41,42], resulting in continuous oxygen release. Long-term continuous oxygen supply is critical for the survival of transplanted cells in ischemic limbs since angiogenesis typically requires more than 3 weeks to establish [37,56,57]. The microspheres were further immobilized with catalase. Successful conjugation was confirmed by confocal image where FITC-labeled catalase was in the shell (Fig. 4C). The catalase loading efficiency was 260 $\mu g_{catalase}/mg_{microsphere}$.

Oxygen was released from the microspheres after the PVP/H_2O_2 complex diffused to the shell was converted by the catalase immobilized on the shell. The oxygen release study was performed at 1% and 5% O_2 conditions, respectively. The oxygen was able to gradually release from the microspheres during the 4-week experimental period (Fig. 5). The release rate was dependent on the NI content in the microspheres, and environment oxygen level. For the microspheres without NI (PNHAN/NI0/CAT), the oxygen release rate was similar during the first 5 days regardless of the environmental oxygen level (Fig. 5). The release at 1% and 5% O_2 conditions peaked at day 14 and day 7 respectively, followed by slower release till day 28. These results demonstrate that the microspheres without NI cannot release oxygen in response to environmental oxygen level. In contrast, the microspheres with NI (PNHAN/NI5/CAT and PNHAN/NI16/CAT) were able to release higher amount of oxygen under 1% O_2 than under 5% O_2 during the 4-week period (Fig. 5, **Appendix. 3**). The microspheres with higher NI content released more oxygen at both oxygen conditions. In PNHAN/NI16/CAT group, the released oxygen level was significantly higher under 1% O_2 than 5% O_2 starting from day 3 ($p < 0.001$). When comparing the oxygen release kinetics of the microspheres with different NI content under the same

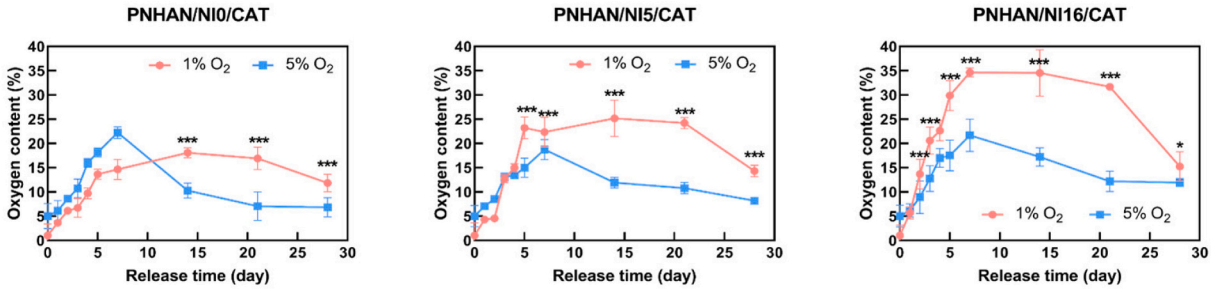

Fig. 5. Oxygen release kinetics. The oxygen release of the microspheres with different NI contents was tested for 28 days under 1% and 5% oxygen content.

oxygen condition, it was found that the release kinetics was similar among the microspheres with different NI content under 5% O_2 condition (**Appendix. 3**). However, under 1% O_2 condition, the oxygen release rate was dependent on the NI content. A higher NI content led to a greater level of released oxygen during the 4-week study period. These results reveal that the microspheres with NI can release oxygen in response to environmental oxygen level. The oxygen release rate for individual NI-containing microsphere type is consistent with water content and degradation results where both were increased under lower oxygen conditions (Fig. 3). The higher water content and faster degradation rate allowed PVP/H_2O_2 complex to diffuse out quicker, leading to faster oxygen release. For the microspheres with different NI content (PNHAN/NI5/CAT and PNHAN/NI16/CAT), the increased water content likely stimulated polymer degradation. The combined effects of water content and degradation rate possibly resulted in accelerated release of oxygen. The hypoxia-sensitive oxygen release is crucial for in vivo applications because the cells in the more hypoxic environment require greater amount of oxygen for their basic metabolism [58]. For the cells in the less ischemic condition, moderate oxygen supply is adequate for their survival and proliferation. An oxygen-release system without hypoxia-sensitivity will cause a universal elevation in oxygen level among all microenvironments. Excessive oxygen will likely cause overproduction of ROS that may have detrimental effect on cells [59].

In this work, the catalase was directly immobilized on microsphere surface (Fig. 4C). To determine whether catalase conjugation affected its bioactivity, the oxygen release from microspheres conjugated with catalase, and from microspheres incubated with free catalase was measured respectively. The microspheres with catalase conjugation released similar amount of oxygen as the microspheres incubated with free catalase on days 1 and 3 (**Appendix. 4,** $p > 0.05$), indicating that the conjugation did not affect catalase bioactivity in converting H_2O_2 into molecular oxygen. One of the advantages of the microspheres with conjugated catalase is that molecular oxygen can be timely and directly released from the microspheres. This avoids released, relatively high concentration of H_2O_2 to contact with transplanted cells and damage them. Most of current oxygen release biomaterials release H_2O_2 first, and the oxygen release is dependent on H_2O_2 decomposition [32,33]. The undecomposed H_2O_2 may interact with cells causing cell death. These microspheres were also advantageous than our previously developed oxygen release system where catalase was mixed with the oxygen-release microspheres in the hydrogel [41,42]. Catalase may release from the hydrogel. The released H_2O_2 may not be timely converted into oxygen when the amount of catalase in the hydrogel is low. In this work, the immobilized catalase efficiently converted the released H_2O_2 into oxygen. During the 4-week release study period, the release medium contained less than 10 μM H_2O_2 as measured by a peroxide assay kit. This concentration is too low to trigger cell apoptosis [60,61].

3.3. *Effect of oxygen-release microspheres on MSC survival under hypoxic condition*

The survival of transplanted MSCs in ischemic environment is pivotal for ischemic limb regeneration [9,62]. To investigate whether the oxygen released from microspheres can improve MSC survival under hypoxia, we loaded MSCs and oxygen-release microspheres together in the PNHA gel. This hydrogel has been confirmed to be injectable and biocompatible [41,51]. The constructs were cultured under hypoxic condition (1% O_2) without supplement of FBS. In the constructs without oxygen-release microspheres (Gel), MSCs experienced extensive death as the dsDNA content largely decreased during the 28-day culture period (Fig. 6A). At day 28, dsDNA content was less than 25% of that at day 1. In the constructs supplemented with oxygen-release microspheres (Gel/PNHAN/NI0/CAT, Gel/PNHAN/NI5/CAT and Gel/PNHAN/NI16/CAT), the released oxygen rescued the cells and even supported their proliferation (Fig. 6A). The dsDNA content did not decrease and/or increased over 4 weeks. This is likely due to the elevation in cellular oxygen content by released oxygen. The constructs containing microspheres with lower NI content (Gel/PNHAN/NI5/CAT) exhibited substantially higher dsDNA content than those containing microspheres without NI (Gel/PNHAN/NI0/CAT). Further increase of NI content significantly increased dsDNA content at each time point ($p < 0.001$, Gel/PNHAN/NI5/CAT vs. Gel/PNHAN/NI16/CAT). The live cell images confirmed the dsDNA results (Fig. 6B). These results are in accordance with the oxygen release kinetics where higher oxygen release amount more greatly improved cell survival.

To understand the mechanism that released oxygen enhanced MSC survival under hypoxia, oxygen content in MSCs was measured using EPR. The MSCs encapsulated in the PNHA gel without oxygen-release microspheres had an oxygen content of 4.2% after 48 h of culture under 1% O_2. The oxygen content was significantly increased to 10.4% when the MSCs were encapsulated in the PNHA gel with oxygen-release microspheres (Fig. 6C, $p < 0.001$). These results demonstrate that the enhanced cell survival under hypoxia was resulted from increased intracellular oxygen content. It remains to be investigated whether the released oxygen changes cell metabolic behaviors, such as oxygen consumption rate, glycolysis rate and fatty acid oxidation under hypoxia.

One of the concerns for released oxygen is that it may increase ROS content in MSCs leading to cell death. To determine ROS content in the cells, CM-H_2DCFDA staining was performed (**Appendix. 5**). At days 1, 14 and 28, the groups with oxygen-release microspheres exhibited similar ROS content (Fig. 6D). Interestingly, the ROS content was significantly lower than that in the group without oxygen release ($p < 0.05$ or 0.001). These results demonstrate that the released oxygen did not raise the oxidative stress in MSCs. There was no significant difference between O_2-sensitive and insensitive microspheres in ROS production under hypoxia ($p > 0.05$). It is possible that the oxygen released from these microspheres was consumed by metabolic-demanding MSCs for survival under hypoxia instead of generating ROS.

Since PNHAN/NI16/CAT microspheres had the fastest oxygen release, most significantly promoted MSC survival under ischemic condition, and did not induce oxidative stress, they were used in vivo to investigate whether the implantation of MSCs and oxygen-release microspheres can promote cell survival and tissue regeneration in ischemic limbs.

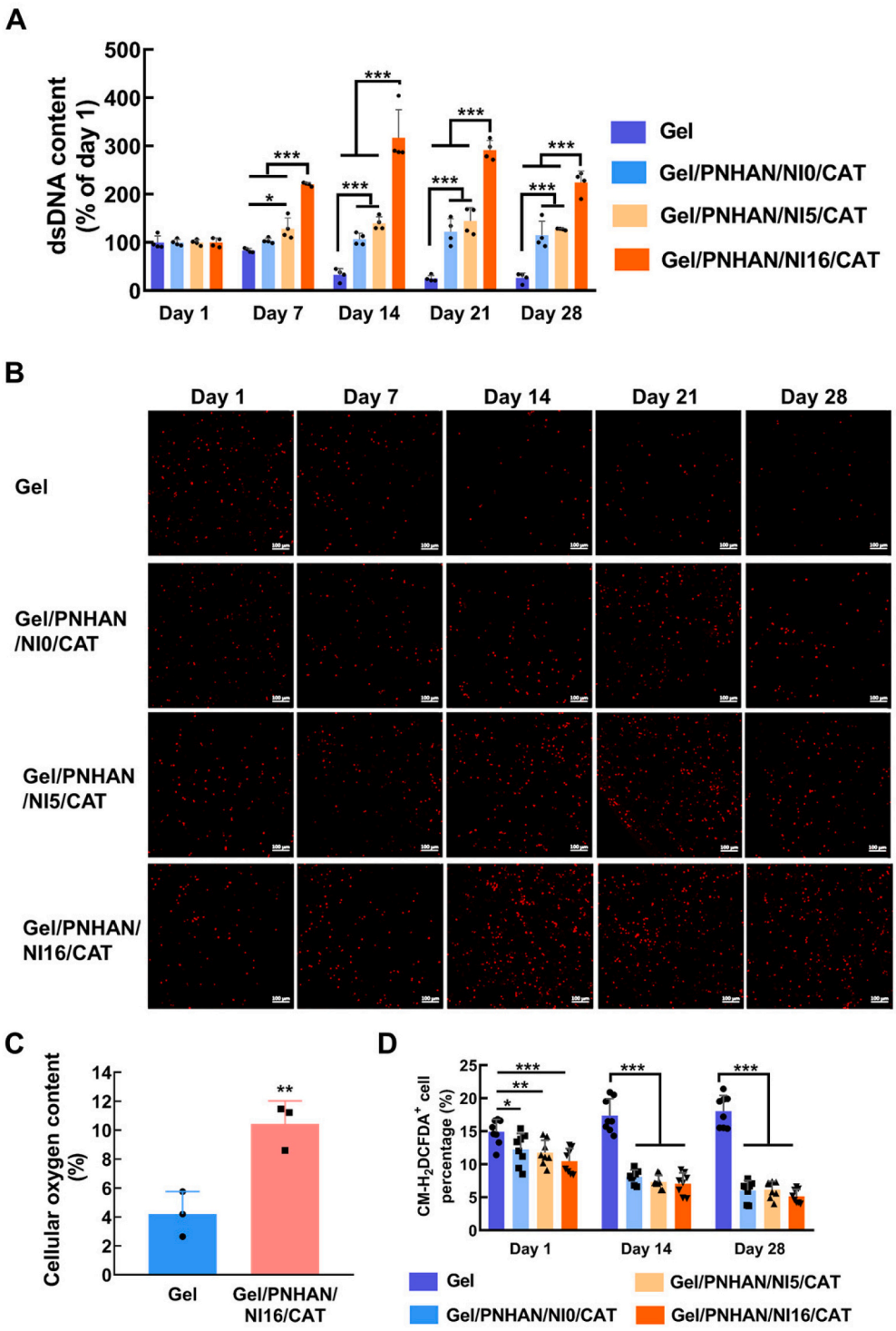

Fig. 6. Effect of oxygen-release microspheres on MSC survival and ROS production under hypoxia. (A) dsDNA content of MSCs encapsulated in PNHA gel with and without oxygen-release microspheres during 28 days of culture; (B) Fluorescent images of live MSCs encapsulated in PNHA gel with and without oxygen-release microspheres during 28 days of culture; (C) Cellular oxygen content measurement of MSCs encapsulated in PNHA gel with and without microspheres after 48 h; (D) ROS content expressed by MSCs encapsulated in PNHA gel with and without oxygen-release microspheres during 28 days of culture. $^{*}p < 0.05$, $^{**}p < 0.01$, $^{***}p < 0.001$.

3.4. *Effect of oxygen release on MSC survival and paracrine effects in ischemic limbs*

To determine whether the oxygen-release microspheres (ORM) can increase MSC survival in ischemic limbs, the microspheres and live cell tracker CM-Dil-labeled MSCs were encapsulated in the PNHA gel, and injected into thigh muscles. Four weeks after implantation, live MSCs were imaged. The number of CMDil+ MSCs was apparently much higher in the Gel/MSC/ORM group than in the Gel/MSC group (Fig. 7A**&B**). The quantitative live MSC density of the Gel/MSC/ORM group was more than 3 times of the Gel/MSC group ($p < 0.001$). Based on the in vitro results that the released oxygen increased MSC intracellular oxygen content (Fig. 6C), it is likely that the oxygen released in vivo also augmented intracellular oxygen content in the transplanted MSCs, leading to enhanced cell survival. The oxygen content either in the MSCs or ischemic tissues remains to be measured since current techniques cannot non-invasively and long-term detect tissue oxygen content.

To determine whether the released oxygen enhanced MSC proliferation in the ischemic limbs, Ki67 staining was performed (Fig. 7C). The Ki67+/CMDil+ cells were identified as proliferating MSCs. The cell density in the Gel/MSC/ORM group was raised more than 4-fold compared to that in the Gel/MSC group ($p < 0.001$, Fig. 7D),

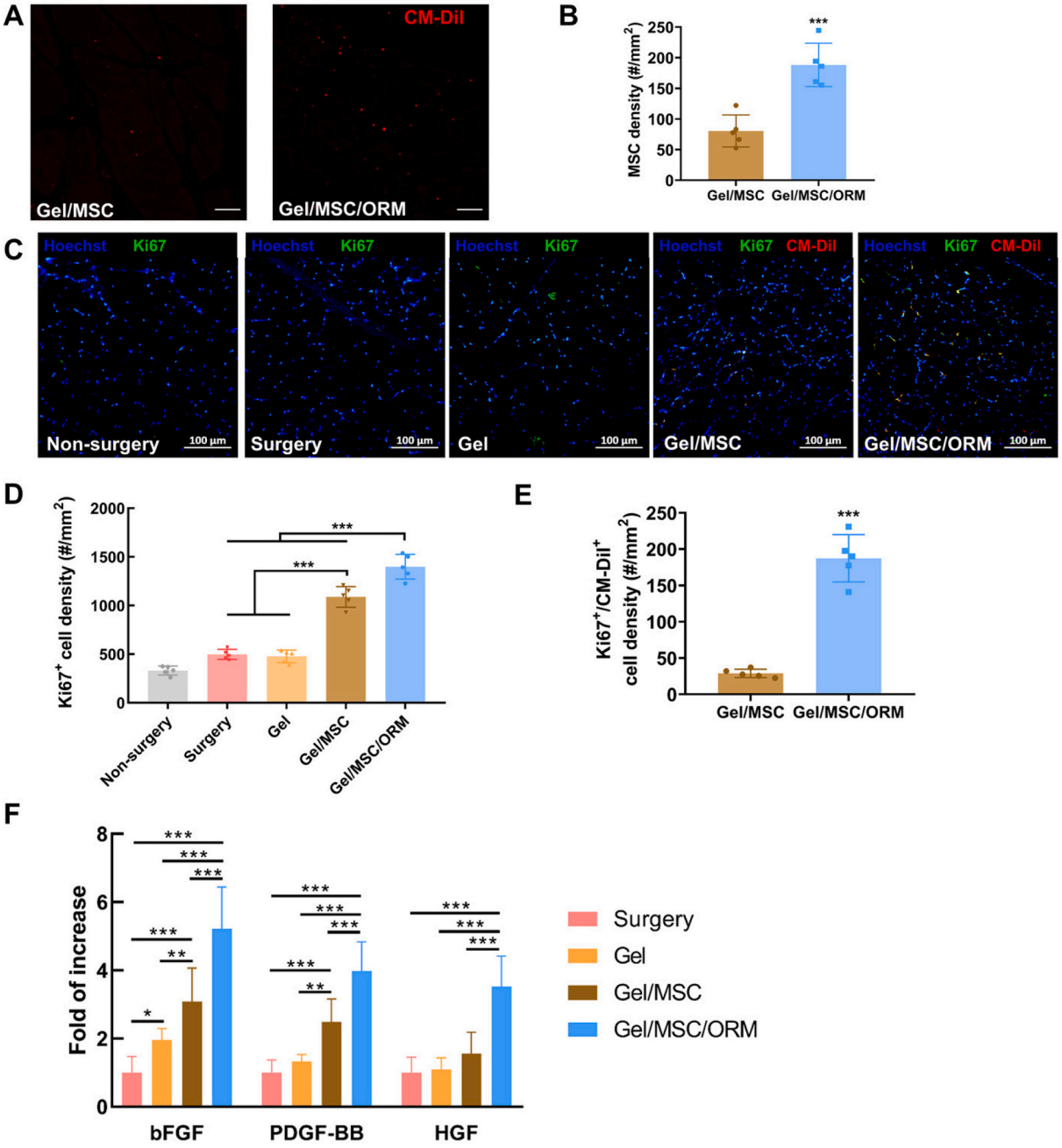

Fig. 7. In vivo MSC survival, proliferation and paracrine effect. (A) Fluorescent images of MSCs in ischemic limbs 28 days after implantation. MSCs were pre-labeled with live cell track CM-Dil (red) before implantation. Scale bar = 50 μm; (B) MSC density in ischemic limbs 28 days after implantation; (C) Immunohistochemical staining of Ki67 (green) of limb tissue sections 28 days after CLI surgery. Nuclei were stained with Hoechst 33342 (blue) and MSCs were pre-labeled with CM-Dil (red) before implantation; (D) Quantification of overall Ki67+ cell density in ischemic limbs. The Ki67+ cells were proliferating cells; (E) Quantification of Ki67+/CM-Dil + cell density. The Ki67+/CM-Dil + cells were proliferating MSCs that were transplanted into ischemic limbs; (F) Expression of bFGF, PDGF-BB and HGF in ischemic limb tissues 28 days after surgery. $*p < 0.05$, $**p < 0.01$, $***p < 0.001$. (For interpretation of the references to colour in this figure legend, the reader is referred to the web version of this article.)

demonstrating that the released oxygen promoted MSC proliferation besides survival. The Gel/MSC/ORM group also had significantly greater overall proliferating cell density than the Gel/MSC group ($p < 0.001$, Fig. 7E). It is possible that the released oxygen also improved host cell survival. This is consistent with our previous study where delivery of oxygen into ischemic hearts ameliorated cardiac cell survival [41]. Notably, the groups with MSCs exhibited more abundant Ki67 expression than the groups without MSCs (Surgery and Gel groups, Fig. 7 **C & D**), illuminating that the survived MSCs played an important role to the host cell survival.

MSCs are known to promote cell survival and tissue regeneration mainly by paracrine effects [63]. To determine how MSC paracrine effects were expressed in the ischemic limbs, the prosurvival growth factor expressions were quantified at the mRNA level at day 28. Among different prosurvival growth factors, the bFGF and PDGF-BB expressions were significantly increased in the Gel/MSC and Gel/MSC/ORM groups compared with Surgery and Gel groups (Fig. 7F). It is possible that these growth factors promoted host cell survival. The Gel/MSC/ORM group exhibited significantly higher bFGF and PDGF-BB expressions than the Gel/MSC group ($p < 0.001$). Besides bFGF and PDGFBB, the Gel/MSC/

ORM group also had significantly greater HGF expression ($p < 0.001$), whereas the Gel/MSC, Surgery and Gel groups had similar expression ($p > 0.05$). The above results reveal that the released oxygen significantly promoted MSC paracrine effects. Stem cell paracrine effects are dependent on the oxygen level. Studies have shown that a relatively low oxygen condition (5–20%) may increase cell paracrine effects [64–68]. However, an extremely low oxygen condition (<1%) largely decreases paracrine effects [69]. Our results demonstrate that the amount of released oxygen was in the range that increases MSC paracrine effects.

3.5. Efficacy of oxygen-release microspheres and MSCs in promoting vascularization in ischemic limb

To determine whether enhanced MSC survival and paracrine effect, and increased host cell survival accelerated tissue vascularization, blood perfusion in the ischemic limbs was monitored by Laser Doppler, and blood vessels were characterized by immunohistology. The blood perfusion in the Surgery group was slowly increased during the 4-week experimental period with 41% blood perfusion at week 4 (Fig. 8 **A & B**). The injection of PNHA gel only (Gel group) did not significantly enhance the blood perfusion. In contrast, the encapsulation of MSCs in the hydrogel (Gel/MSC group) significantly increased blood perfusion compared to Gel group at days 14, 21 and 28 ($p < 0.05$). The fastest blood flow recovery was found for the Gel/MSC/ORM group where both MSCs and oxygen-release microspheres were encapsulated in the hydrogel (Fig. 8 **A & B**). The blood perfusion was ~90% of that of the normal limb at day 28. The blood flow result proved that the incorporation of microspheres could enhance the survival of MSCs and host cells under ischemia. These results demonstrate that enhanced MSC survival and paracrine effects, and host cell survival accelerated tissue vascularization.

To visualize the blood vessels in ischemic limbs, isolectin and αSMA stainings were performed for tissues harvested at day 28 (Fig. 8C). Consistent with blood perfusion results, the implantation of Gel/MSC significantly increased the blood vessel density than the Surgery and Gel groups ($p < 0.001$, Fig. 8D). The implantation of Gel/MSC/ORM further increased vessel density to 90% of that of the normal limbs (Fig. 8D). The co-delivery of MSCs and oxygen-release microspheres also largely promoted vessel maturation. The isolectin+/αSMA+ mature vessel density was significantly higher than the delivery of MSCs only (Fig. 8E). As the transplanted MSCs did not differentiate into isolectin+ endothelial cells or αSMA+ smooth muscle cells, the enhanced vascularization is likely resulted from upregulated bFGF, PDGF-BB, and HGF expressions (Fig. 7F). These growth factors have angiogenic effect [7,55,70]. The upregulated PDGF-BB can also recruit smooth muscle cells to stimulate vessel maturation. Besides paracrine effects, MSCs may also stabilize blood vessels by acting as pericytes [25–27]. It remains to be investigated whether delivery of MSCs and oxygen-release microspheres promoted the formation of functional vessels in ischemic limbs, which can be determined by performing vascular perfusion with fluorescent-labeled lectin following by visualizing the functional blood vessels.

3.6. Effect of oxygen-release microspheres and MSCs on skeletal muscle regeneration and tissue inflammation in ischemic limbs

Vascularization and myogenesis are two goals for ischemic tissue regeneration. Previous studies have demonstrated that myogenesis

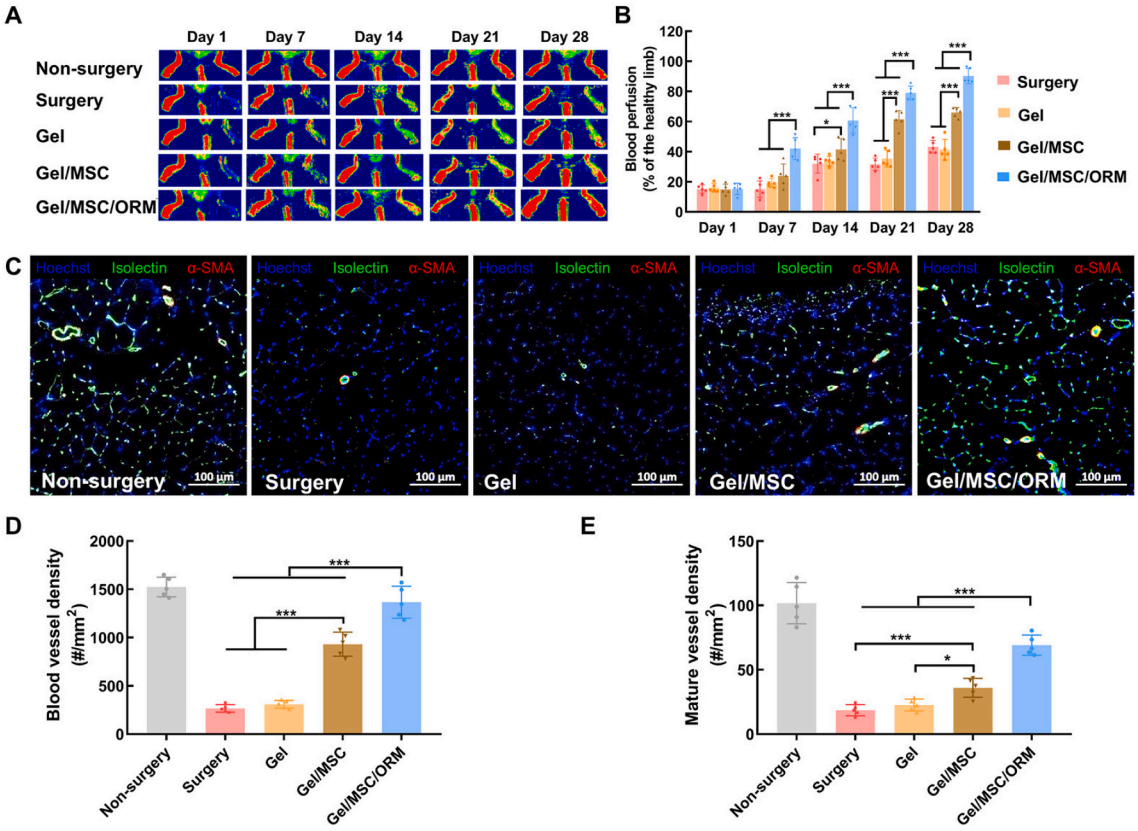

Fig. 8. Delivery of oxygen-release microspheres and MSCs promoted tissue angiogenesis. (A) Laser Doppler perfusion images of non-surgery group and surgery groups with different treatments for 28 days; (B) Blood perfusion of ischemic limbs for 28 days. The results were normalized to the non-surgery limb for each animal; (C) Immunohistochemical staining of isolectin (green) and α-SMA (red) of limb tissue sections 28 days after CLI surgery. Nuclei were stained with Hoechst 33342 (blue); (D) Quantification of total blood vessel density; (E) Quantification of mature blood vessel density. *$p < 0.05$, ***$p < 0.001$. (For interpretation of the references to colour in this figure legend, the reader is referred to the web version of this article.)

largely depends on vascularization [71]. To determine myogenesis in the ischemic limbs, H&E and MHC stainings were used (Fig. 9 **A & B**). In the Surgery and Gel groups, the skeletal muscle was degenerated as the muscle fibers were highly isolated (Fig. 9 **A & B**). The injection of Gel/MSC and Gel/MSC/ORM promoted skeletal muscle regeneration, as the muscle fiber diameter was significantly increased compared to the Surgery and Gel groups ($p < 0.001$. Fig. 9C). The Gel/MSC/ORM group exhibited significantly larger muscle fiber diameter than the Gel/MSC group ($p < 0.001$. Fig. 9C). In addition, the blood vessel distribution in the muscle fibers was similar to that in the healthy hindlimbs (Fig. 9B). Regenerating skeletal muscle contains central nucleus [72]. Consistent with muscle fiber results, the central nucleus density was remarkably greater in the Gel/MSC/ORM group than other groups (Fig. 9D). The above results demonstrate that co-delivery of MSCs and oxygen-release microspheres significantly promoted skeletal muscle regeneration. It is speculated that the enhanced MSC paracrine effects, and improved survival of skeletal muscle cells by released oxygen accelerated myogenesis. It is also possible that the MSC paracrine effects activated muscle resident stem cells to proliferate and differentiate to form new myofibers [73].

The implantation of MSCs, oxygen-release microspheres and PNHA hydrogel may lead to immune response and inflammation. Excessive inflammation has been shown to inhibit the activation of the quiescent population of muscle-resident stem cells for skeletal muscle regeneration [73]. F4/80 staining was used to investigate tissue inflammation (Fig. 10). Compared with the Non-surgery group, the Surgery group had a significantly higher density of F4/80+ macrophages. The injection of Gel group, Gel/MSC group, and Gel/MSC/ORM group did not augment tissue inflammation as these groups had similar density of F4/80+ macrophages as the Surgery group ($p > 0.05$). These results demonstrate that the PNHA and oxygen-release microspheres had excellent biocompatibility.

The above results demonstrate that the oxygen-release microspheres with hypoxia sensitivity were able to release oxygen in response to environmental oxygen level. The released oxygen increased cell survival under ischemia while avoiding excessive oxygenation that may cause ROS formation and inflammation. Various studies have shown that excessive oxygenation leads to ischemia/reperfusion injury, characterized by high oxidative stress and inflammation [74–80]. The oxygen-release microspheres in this work have the potential to reduce ischemia/reperfusion injury.

4. Conclusion

In this study, oxygen-release microspheres whose oxygen release kinetics was responsive to environmental oxygen level were developed. The microspheres released oxygen faster in the lower oxygen environment, and slower in the higher oxygen environment. The released oxygen improved MSC survival without elevating oxidative stress in vitro. In the ischemic limbs, the oxygen-release microspheres significantly

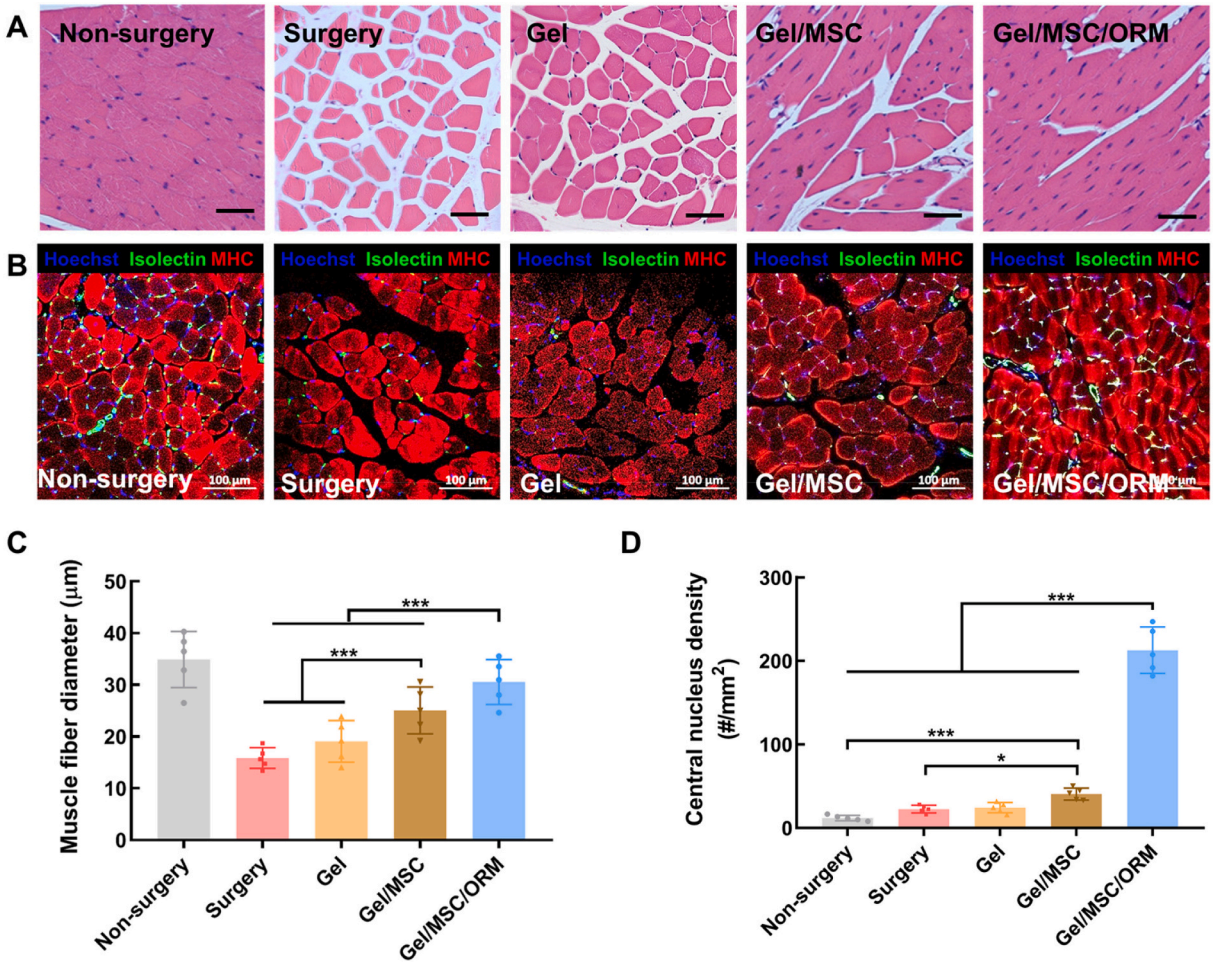

Fig. 9. Delivery of oxygen-release microspheres and MSCs enhanced skeletal muscle regeneration. (A) H&E staining of limb tissue sections 28 days after CLI surgery. Scale bar = 50 μm; (B) Immunohistochemical staining of MHC (red) and isolectin (green) of limb tissue sections 28 days after CLI surgery. Nuclei were stained with Hoechst 33342 (blue); (C) Quantification of muscle fiber diameter; (D) Quantification of central nucleus density. *$p < 0.05$, ***$p < 0.001$. (For interpretation of the references to colour in this figure legend, the reader is referred to the web version of this article.)

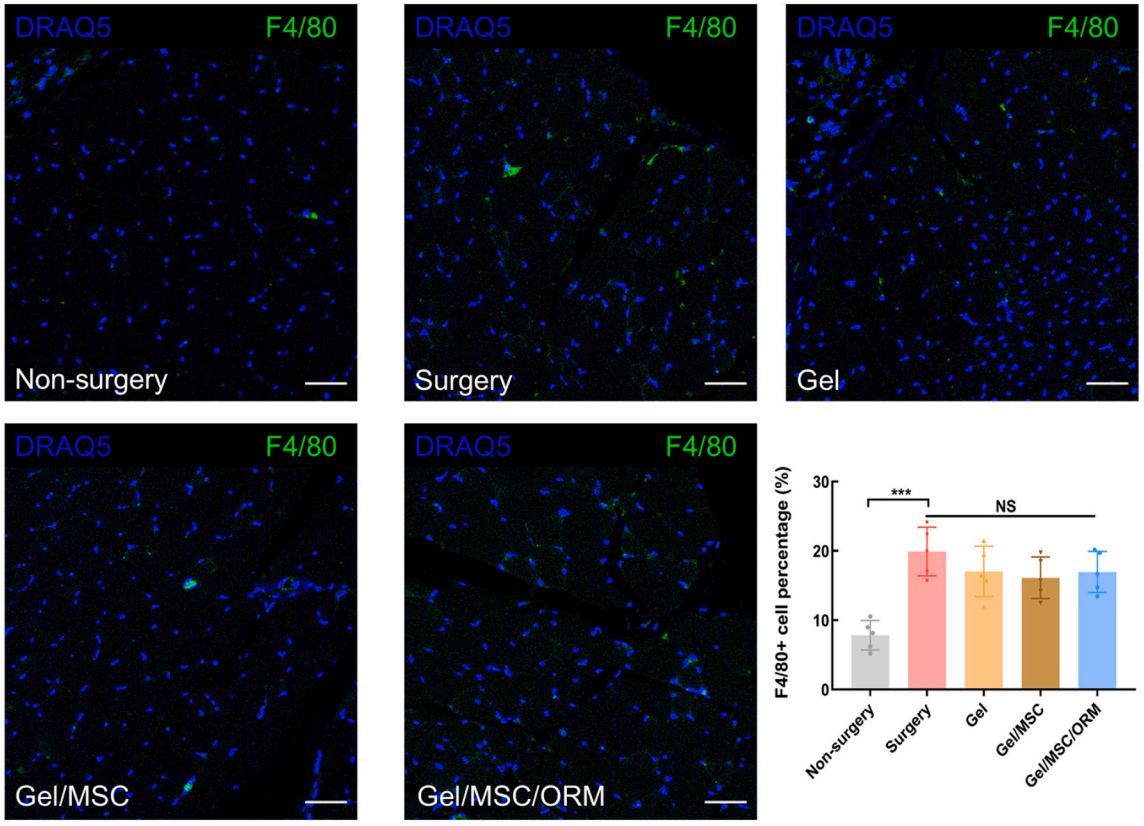

Fig. 10. Biocompatibility of the oxygen-release microspheres. Immunohistochemical staining of F4/80 (green) of limb tissue sections 28 days after CLI surgery and the quantification of F4/80 positive cell percentage. Nuclei were stained with DRAQ5 (blue). Scale bar = 50 μm. (For interpretation of the references to colour in this figure legend, the reader is referred to the web version of this article.)

improved MSC survival, proliferation and paracrine effects, and host cell survival, leading to accelerated tissue vascularization and skeletal muscle regeneration. The microspheres possessed excellent biocompatibility. These microspheres provided a smart way of delivering oxygen to ischemic tissues to enhance exogenous and endogenous cell survival. The environment-responsive oxygen release can avoid excessive oxygen release that may increase oxidative stress and cause cell death.

Credit author statement

YG, NG and JG developed ideas. YG, NG, HN and YD performed experiments. YG, NG and JG wrote manuscript.

Acknowledgement

This work was supported by US National Institutes of Health (R01HL138175, R01HL138353, R01EB022018, R01AG056919, and R01AR077616), and National Science Foundation (1922857).

Appendix A. Supplementary data

Supplementary data to this article can be found online at https://doi.org/10.1016/j.jconrel.2021.01.034.

References

[1] F. Sanada, Y. Taniyama, J. Muratsu, R. Otsu, H. Shimizu, H. Rakugi, et al., Gene-therapeutic strategies targeting angiogenesis in peripheral artery disease, Medicines 5 (2018) 31.
[2] P. Barć, M. Antkiewicz, B. Śliwa, D. Baczyńska, W. Witkiewicz, J.P. Skóra, Treatment of critical limb ischemia by pIRES/VEGF165/HGF Administration, Ann. Vasc. Surg. 60 (2019) 346–354.
[3] W. Leppert, R. Zajaczkowska, J. Wordliczek, J. Dobrogowski, J. Woron, M. Krzakowski, Pathophysiology and clinical characteristics of pain in most common locations in cancer patients, J. Physiol. Pharmacol. 67 (2016) 787–799.
[4] C.N. Hess, L. Norgren, G.M. Ansel, W.H. Capell, J.P. Fletcher, F.G.R. Fowkes, et al., A structured review of antithrombotic therapy in peripheral artery disease with a focus on revascularization: a TASC (InterSociety consensus for the Management of Peripheral Artery Disease) initiative, Circulation 135 (2017) 2534–2555.
[5] L. Uccioli, M. Meloni, V. Izzo, L. Giurato, S. Merolla, R. Gandini, Critical limb ischemia: current challenges and future prospects, Vasc. Health Risk Manag. 14 (2018) 63–74.
[6] M. Hassanshahi, S. Khabbazi, Y. Peymanfar, A. Hassanshahi, Z. Hosseini-Khah, Y. W. Su, et al., Critical limb ischemia: current and novel therapeutic strategies, J. Cell. Physiol. 234 (2019) 14445–14459.
[7] G.O. Ouma, B. Zafrir, E.R. Mohler III, M.Y. Flugelman, Therapeutic angiogenesis in critical limb ischemia, Angiology 64 (2013) 466–480.
[8] F. Sanada, Y. Taniyama, J. Azuma, I.-I. Yuka, Y. Kanbara, M. Iwabayashi, et al., Therapeutic angiogenesis by gene therapy for critical limb ischemia: choice of biological agent, in: Immunology, Endocrine & Metabolic Agents in Medicinal Chemistry (Formerly Current Medicinal Chemistry-Immunology, Endocrine and Metabolic Agents) 14, 2014, pp. 32–39.
[9] M. Qadura, D.C. Terenzi, S. Verma, M. Al-Omran, D.A. Hess, Concise review: cell therapy for critical limb ischemia: an integrated review of preclinical and clinical studies, Stem Cells 36 (2018) 161–171.
[10] E. Tateishi-Yuyama, H. Matsubara, T. Murohara, U. Ikeda, S. Shintani, H. Masaki, et al., Therapeutic angiogenesis for patients with limb ischaemia by autologous transplantation of bone-marrow cells: a pilot study and a randomised controlled trial, Lancet 360 (2002) 427–435.
[11] R. Al-Rifai, P. Nguyen, N. Bouland, C. Terryn, L. Kanagaratnam, G. Poitevin, et al., In vivo efficacy of endothelial growth medium stimulated mesenchymal stem cells derived from patients with critical limb ischemia, J. Transl. Med. 17 (2019) 261.
[12] M.G. MacAskill, J. Saif, A. Condie, M.A. Jansen, T.J. MacGillivray, A.A. Tavares, et al., Robust revascularization in models of limb ischemia using a clinically translatable human stem cell-derived endothelial cell product, Mol. Ther. 26 (2018) 1669–1684.
[13] K.J. Portalska, A. Leferink, N. Groen, H. Fernandes, L. Moroni, C. van Blitterswijk, et al., Endothelial differentiation of mesenchymal stromal cells, PLoS One 7 (2012), e46842.
[14] K. Zhi, Z. Gao, J. Bai, Y. Wu, S. Zhou, M. Li, et al., Application of adipose-derived stem cells in critical limb ischemia, Frontiers in bioscience 19 (2014) 768–776 (Landmark edition).

[15] X. Wang, J. Zhang, W. Cui, Y. Fang, L. Li, S. Ji, et al., Composite hydrogel modified by IGF-1C domain improves stem cell therapy for limb ischemia, ACS Appl. Mater. Interfaces 10 (2018) 4481–4493.
[16] L. Debin, J. Youzhao, L. Ziwen, L. Xiaoyan, Z. Zhonghui, C. Bing, Autologous transplantation of bone marrow mesenchymal stem cells on diabetic patients with lower limb ischemia, J. Med. Coll. PLA 23 (2008) 106–115.
[17] P.A. Tebebi, S.J. Kim, R.A. Williams, B. Milo, V. Frenkel, S.R. Burks, et al., Improving the therapeutic efficacy of mesenchymal stromal cells to restore perfusion in critical limb ischemia through pulsed focused ultrasound, Sci. Rep. 7 (2017) 41550.
[18] A. Liew, T. O'Brien, Therapeutic potential for mesenchymal stem cell transplantation in critical limb ischemia, Stem Cell Res Ther 3 (2012) 28.
[19] Q. Lian, Y. Zhang, J. Zhang, H.K. Zhang, X. Wu, Y. Zhang, et al., Functional mesenchymal stem cells derived from human induced pluripotent stem cells attenuate limb ischemia in mice, Circulation 121 (2010) 1113–1123.
[20] A. Abdal Dayem, S.B. Lee, K. Kim, K.M. Lim, Jeon T-i, J. Seok, et al., Production of Mesenchymal Stem Cells through Stem Cell Reprogramming, International journal of molecular sciences 20 (2019) 1922.
[21] P. Yan, Q. Li, L. Wang, P. Lu, K. Suzuki, Z. Liu, et al., FOXO3-engineered human ESC-derived vascular cells promote vascular protection and regeneration, Cell stem cell 24 (2019) 447–461, e8.
[22] Y. Fujita, A. Kawamoto, Stem cell-based peripheral vascular regeneration, Adv. Drug Deliv. Rev. 120 (2017) 25–40.
[23] V. Gorenoi, M.U. Brehm, A. Koch, A. Hagen, Growth factors for angiogenesis in peripheral arterial disease, in: Cochrane Database of Systematic Reviews, 2017.
[24] M.E. Bernardo, W.E. Fibbe, Mesenchymal stromal cells: sensors and switchers of inflammation, Cell Stem Cell 13 (2013) 392–402.
[25] K. Gaengel, G. Genové, A. Armulik, C. Betsholtz, Endothelial-mural cell signaling in vascular development and angiogenesis, Arterioscler. Thromb. Vasc. Biol. 29 (2009) 630–638.
[26] A. Blocki, Y. Wang, M. Koch, P. Peh, S. Beyer, P. Law, et al., Not all MSCs can act as pericytes: functional in vitro assays to distinguish pericytes from other mesenchymal stem cells in angiogenesis, Stem Cells Dev. 22 (2013) 2347–2355.
[27] M. Crisan, S. Yap, L. Casteilla, C.W. Chen, M. Corselli, T.S. Park, et al., A perivascular origin for mesenchymal stem cells in multiple human organs, Cell Stem Cell 3 (2008) 301–313.
[28] D.P. Sieveking, M.K. Ng, Cell therapies for therapeutic angiogenesis: back to the bench, Vasc. Med. 14 (2009) 153–166.
[29] F. Hached, C. Vinatier, C. Le Visage, H. Gondé, J. Guicheux, G. Grimandi, et al., Biomaterial-assisted cell therapy in osteoarthritis: from mesenchymal stem cells to cell encapsulation, Best Pract. Res. Clin. Rheumatol. 31 (2017) 730–745.
[30] N.K. Gupta, E.J. Armstrong, S.A. Parikh, The current state of stem cell therapy for peripheral artery disease, Curr. Cardiol. Rep. 16 (2014) 447.
[31] X.L. Aranguren, C.M. Verfaillie, A. Luttun, Emerging hurdles in stem cell therapy for peripheral vascular disease, J. Mol. Med. 87 (2009) 3.
[32] S.E. Bae, J.S. Son, K. Park, D.K. Han, Fabrication of covered porous PLGA microspheres using hydrogen peroxide for controlled drug delivery and regenerative medicine, J. Control. Release 133 (2009) 37–43.
[33] S.-M. Ng, J.-Y. Choi, H.-S. Han, J.-S. Huh, J.O. Lim, Novel microencapsulation of potential drugs with low molecular weight and high hydrophilicity: hydrogen peroxide as a candidate compound, Int. J. Pharm. 384 (2010) 120–127.
[34] S.H. Oh, C.L. Ward, A. Atala, J.J. Yoo, B.S. Harrison, Oxygen generating scaffolds for enhancing engineered tissue survival, Biomaterials 30 (2009) 757–762.
[35] K. Chin, S.F. Khattak, S.R. Bhatia, S.C. Roberts, Hydrogel-perfluorocarbon composite scaffold promotes oxygen transport to immobilized cells, Biotechnol. Prog. 24 (2008) 358–366.
[36] A. Wijekoon, N. Fountas-Davis, N.D. Leipzig, Fluorinated methacrylamide chitosan hydrogel systems as adaptable oxygen carriers for wound healing, Acta Biomater. 9 (2013) 5653–5664.
[37] J. Chal, O. Pourquié, Making muscle: skeletal myogenesis in vivo and in vitro, Development 144 (2017) 2104–2122.
[38] B.H. Annex, Therapeutic angiogenesis for critical limb ischaemia, Nat. Rev. Cardiol. 10 (2013) 387.
[39] I.E. Hoefer, N. van Royen, I.R. Buschmann, J.J. Piek, W. Schaper, Time course of arteriogenesis following femoral artery occlusion in the rabbit, Cardiovasc. Res. 49 (2001) 609–617.
[40] P.I. Makarevich, M.A. Boldyreva, E.V. Gluhanyuk, A.Y. Efimenko, K.V. Dergilev, E. K. Shevchenko, et al., Enhanced angiogenesis in ischemic skeletal muscle after transplantation of cell sheets from baculovirus-transduced adipose-derived stromal cells expressing VEGF165, Stem Cell Research Therapy 6 (2015) 204.
[41] Z. Fan, Z. Xu, H. Niu, N. Gao, Y. Guan, C. Li, et al., An injectable oxygen release system to augment cell survival and promote cardiac repair following myocardial infarction, Sci. Rep. 8 (2018) 1371.
[42] Z. Li, X. Guo, J. Guan, An oxygen release system to augment cardiac progenitor cell survival and differentiation under hypoxic condition, Biomaterials 33 (2012) 5914–5923.
[43] Y. Guan, H. Niu, Y. Dang, N. Gao, J. Guan, Photoluminescent oxygen-release microspheres to image the oxygen release process in vivo, Acta Biomater. 115 (2020) 333–342.
[44] T.M. Buttke, P.A. Sandstrom, Oxidative stress as a mediator of apoptosis, Immunology Today 15 (1994) 7.
[45] H. Fujita, I. Morita, Murota S-i, Hydrogen peroxide induced apoptosis of endothelial cells concomitantly with cycloheximide, J. Atheroscler. Thromb. 7 (2000) 209–215.
[46] M. Singh, H. Sharma, N. Singh, Hydrogen peroxide induces apoptosis in HeLa cells through mitochondrial pathway, Mitochondrion 7 (2007) 367–373.
[47] J. Xiang, C. Wan, R. Guo, D. Guo, Is hydrogen peroxide a suitable apoptosis inducer for all cell types? Biomed. Res. Int. 2016 (2016).
[48] S. Kizaka-Kondoh, H. Konse-Nagasawa, Significance of nitroimidazole compounds and hypoxia-inducible factor-1 for imaging tumor hypoxia, Cancer Sci. 100 (2009) 1366–1373.
[49] J. Yu, Y. Zhang, Y. Ye, R. DiSanto, W. Sun, D. Ranson, et al., Microneedle-array patches loaded with hypoxia-sensitive vesicles provide fast glucose-responsive insulin delivery, Proc. Natl. Acad. Sci. 112 (2015) 8260–8265.
[50] M. Gülden, A. Jess, J. Kammann, E. Maser, H. Seibert, Cytotoxic potency of H2O2 in cell cultures: impact of cell concentration and exposure time, Free Radic. Biol. Med. 49 (2010) 1298–1305.
[51] Z. Fan, Z. Xu, H. Niu, Y. Sui, H. Li, J. Ma, et al., Spatiotemporal delivery of basic fibroblast growth factor to directly and simultaneously attenuate cardiac fibrosis and promote cardiac tissue vascularization following myocardial infarction, J. Control. Release 311 (2019) 233–244.
[52] H. Niu, C. Li, Y. Guan, Y. Dang, X. Li, Z. Fan, et al., High oxygen preservation hydrogels to augment cell survival under hypoxic condition, Acta Biomaterialia 105 (2020) 56–67.
[53] H. Niu, X. Li, H. Li, Z. Fan, J. Ma, J. Guan, Thermosensitive, fast gelling, photoluminescent, highly flexible, and degradable hydrogels for stem cell delivery, Acta Biomater. 83 (2019) 96–108.
[54] M. Quaranta, S.M. Borisov, I. Klimant, Indicators for optical oxygen sensors, Bioanal. Rev. 4 (2012) 115–157.
[55] Y. Xu, M. Fu, Z. Li, Z. Fan, X. Li, Y. Liu, et al., A prosurvival and proangiogenic stem cell delivery system to promote ischemic limb regeneration, Acta Biomater. 31 (2016) 99–113.
[56] A. Uccelli, T. Wolff, P. Valente, N. Di Maggio, M. Pellegrino, L. Gürke, et al., Vascular endothelial growth factor biology for regenerative angiogenesis, Swiss Med. Wkly. 149 (2019).
[57] J.E. Markkanen, T.T. Rissanen, A. Kivelä, S. Ylä-Herttuala, Growth factor-induced therapeutic angiogenesis and arteriogenesis in the heart–gene therapy, Cardiovasc. Res. 65 (2005) 656–664.
[58] G. Solaini, A. Baracca, G. Lenaz, G. Sgarbi, Hypoxia and mitochondrial oxidative metabolism, Biochimica et Biophysica Acta (BBA)-Bioenergetics 1797 (2010) 1171–1177.
[59] M. Redza-Dutordoir, D.A. Averill-Bates, Activation of apoptosis signalling pathways by reactive oxygen species. Biochimica et Biophysica Acta (BBA)-molecular, Cell Res. 1863 (2016) 2977–2992.
[60] A. Cossu, A.M. Posadino, R. Giordo, C. Emanueli, A.M. Sanguinetti, A. Piscopo, et al., Apricot melanoidins prevent oxidative endothelial cell death by counteracting mitochondrial oxidation and membrane depolarization, PLoS One 7 (2012), e48817.
[61] V. Houot, P. Etienne, A.S. Petitot, S. Barbier, J.P. Blein, L. Suty, Hydrogen peroxide induces programmed cell death features in cultured tobacco BY-2 cells, in a dose-dependent manner, J. Exp. Bot. 52 (2001) 1721–1730.
[62] S. Lee, E. Choi, M.-J. Cha, K.-C. Hwang, Cell adhesion and long-term survival of transplanted mesenchymal stem cells: a prerequisite for cell therapy, Oxidative Med. Cell. Longev. 2015 (2015).
[63] H.M. Kwon, S.-M. Hur, K.-Y. Park, C.-K. Kim, Y.-M. Kim, H.-S. Kim, et al., Multiple paracrine factors secreted by mesenchymal stem cells contribute to angiogenesis, Vasc. Pharmacol. 63 (2014) 19–28.
[64] H. Thangarajah, I.N. Vial, E. Chang, S. El-Ftesi, M. Januszyk, E.I. Chang, et al., IFATS collection: Adipose stromal cells adopt a proangiogenic phenotype under the influence of hypoxia, Stem cells (Dayton, Ohio) 27 (2009) 266–274.
[65] J. Rehman, D. Traktuev, J. Li, S. Merfeld-Clauss, C.J. Temm-Grove, J.E. Bovenkerk, et al., Secretion of angiogenic and antiapoptotic factors by human adipose stromal cells, Circulation 109 (2004) 1292–1298.
[66] C.M. Cameron, F. Harding, W.S. Hu, D.S. Kaufman, Activation of hypoxic response in human embryonic stem cell-derived embryoid bodies, Experimental Biology and Medicine (Maywood, NJ) 233 (2008) 1044–1057.
[67] S.C. Hung, R.R. Pochampally, S.C. Chen, S.C. Hsu, D.J. Prockop, Angiogenic effects of human multipotent stromal cell conditioned medium activate the PI3K-Akt pathway in hypoxic endothelial cells to inhibit apoptosis, increase survival, and stimulate angiogenesis, Stem cells (Dayton, Ohio) 25 (2007) 2363–2370.
[68] K. Tamama, H. Kawasaki, S.S. Kerpedjieva, J. Guan, R.K. Ganju, C.K. Sen, Differential roles of hypoxia inducible factor subunits in multipotential stromal cells under hypoxic condition, J. Cell. Biochem. 112 (2011) 804–817.
[69] Y. Xu, M. Fu, Z. Li, Z. Fan, X. Li, Y. Liu, et al., A prosurvival and proangiogenic stem cell delivery system to promote ischemic limb regeneration, Acta Biomater. 31 (2016) 99–113.
[70] R. Cao, E. Bråkenhielm, R. Pawliuk, D. Wariaro, M.J. Post, E. Wahlberg, et al., Angiogenic synergism, vascular stability and improvement of hind-limb ischemia by a combination of PDGF-BB and FGF-2, Nat. Med. 9 (2003) 604–613.
[71] C. Christov, F. Chrétien, R. Abou-Khalil, G. Bassez, G. Vallet, F.-J. Authier, et al., Muscle satellite cells and endothelial cells: close neighbors and privileged partners, Mol. Biol. Cell 18 (2007) 1397–1409.
[72] B. Cadot, V. Gache, E.R. Gomes, Moving and positioning the nucleus in skeletal muscle - one step at a time, Nucleus (Austin, Tex) 6 (2015) 373–381.
[73] A.J. Wagers, I.M. Conboy, Cellular and molecular signatures of muscle regeneration: current concepts and controversies in adult myogenesis, Cell 122 (2005) 659–667.
[74] J. Lutz, K. Thürmel, U. Heemann, Anti-inflammatory treatment strategies for ischemia/reperfusion injury in transplantation, J. Inflamm. 7 (2010) 1–8.
[75] W. Yao, L.W. Tai, Y. Liu, Z. Hei, H. Li, Oxidative Stress and Inflammation Interaction in Ischemia Reperfusion Injury: Role of Programmed Cell Death, Hindawi, 2019.

[76] M. Sasaki, T. Joh, Inflammation and ischemia-reperfusion injury in gastrointestinal tract and antioxidant, protective agents, J. Clin. Biochem. Nutr. 40 (2007) 1–12.
[77] D.K. de Vries, K.A. Kortekaas, D. Tsikas, L.G. Wijermars, C.J. van Noorden, M.-T. Suchy, et al., Oxidative damage in clinical ischemia/reperfusion injury: a reappraisal, Antioxid. Redox Signal. 19 (2013) 535–545.
[78] G.A. Kurian, R. Rajagopal, S. Vedantham, M. Rajesh, The role of oxidative stress in myocardial ischemia and reperfusion injury and remodeling: revisited, Oxidative Med. Cell. Longev. 2016 (2016).
[79] R.S. Ferrari, C.F. Andrade, Oxidative stress and lung ischemia-reperfusion injury, Oxidative Med. Cell. Longev. 2015 (2015).
[80] M. Kishimoto, J. Suenaga, H. Takase, K. Araki, T. Yao, T. Fujimura, et al., Oxidative stress-responsive apoptosis inducing protein (ORAIP) plays a critical role in cerebral ischemia/reperfusion injury, Sci. Rep. 9 (2019) 1–12.